The Impact of Constitutive Laws on Wellbore Stability: A General Review

P.A. Charlez, SPE, Total Oil Marine

Summary

This paper is focused on soft deep rocks that can induce strong wellbore-stability problems. In the first part, it is shown that these rocks generally exhibit plastic-type behaviors. In the second part two elastoplastic models (Cam-Clay and Laderock) are briefly presented. In the third part, these constitutive laws are applied to wellbore stability through analytical solutions or finite element codes. Finally, in the fourth part, a case history is discussed in detail. We insist on the difficulty to properly define the boundary conditions of the problem (in-situ stresses and virgin pore pressure) and on the subjectivity of the criterion translating the boundary wellbore problem in stability recommendations. Some keys for future research are proposed.

Damaging and Ductile Geomaterials

Materials for which macroscopic rupture[1,2,3] (under deviatoric loading) is preceded by a large linear elastic zone, then by a nonlinear damage zone (**Fig. 1**), are generally considered to be damaging.

The damage phase can be considered a preparation to macroscopic failure, during which progressive development of microcracks parallel to the major stress induces a strong anisotropy[4]. The damage phase is associated with a volumetric dilancy and a reduction of the elastic modulus[5-7] (clearly observed if loading/unloading cycles are performed).

Susceptibility of damaging geomaterials to microcracking and their small capability to strain are mainly caused by a strong cohesion. When the rock is loaded, stresses are concentrated either into the intergranular cement (generally the case for sedimentary rocks) or into the grains themselves, if the mechanical resistance of the cement is higher than that of the grains. The structure will be progressively destroyed by opening and propagation of flaws. The coalescence of these microcracks will finally lead to the collapse of the structure (often a shear band).[8]

Under hydrostatic state of stress, damaging geomaterials do not generally exhibit any type of irreversibility; the behavior remains elastic contractant over a large range of confining pressures. This second property is caused by the good mechanical stability of the porous space, which is again related to the strong cohesion between grains. Consequently, the intrinsic curve of damaging materials is always open upon hydrostatic loading. It is called an open form.

By contrast to damaging materials, ductile rocks[9] can often support large plastic strains (several percent) without any macroscopic failure. From a structural viewpoint, two main petrographic properties differentiate damaging and ductile rocks: a small cohesion and a high porosity. These two properties have determinant consequences on the rheological behavior of the material.

On one part, the high porosity allows ductile materials to be strained irreversibly under hydrostatic loading. The purely contractant-associated plastic mechanism called collapse corresponds to an irreversible reduction of the porosity by implosion of the material.

The plastic collapse mechanism is schematically described in **Fig. 2**. The grains are initially bonded by weak links. Under the effect of an increasing loading, three different phases can be observed. For moderate values of the mean stress (or of the confining pressure), the porous structure remains stable (phase 1) and strain energy (mainly elastic) is stored into the bonds. With the progressive rupture of the bonds, the capability of the material to strain increases and the concavity of the stress/strain curve points downwards. Once free from its bonds, the porous structure collapses, exhibiting very large deformations for only a small increase of the mean stress (phase 2 in Fig. 2). In a third phase, the grains contact with respect to each other. The number of contacts increases, the compressibility of the material decreases, and consequently, the concavity of the stress/strain curve is inverted. In fact, phase 3 corresponds to the common consolidation process that is well-known in soil mechanics. A clear example of such a plastic behavior is presented in **Fig. 3a** (Gorm chalk). For this material, the collapse stress is equal to 20 MPa.

All ductile geomaterials do not necessarily exhibit the three phases described above. For cohesionless materials (no initial bonding between the grains), only the consolidation phase exists. This is often the case for unconsolidated sands (**Fig. 3b**), and also sometimes for shales and claystones.

Under deviatoric loading, and because of small cohesion, these materials are rather insensitive to fissuration. The damage mechanism is replaced by a sliding elastoplastic mechanism between grains mainly governed by internal friction. It very often takes place at constant plastic volume as shown in **Fig. 4**. Of course this second mechanism is coupled with the previous one because contacts between grains resulting from consolidation strongly affect shear failure.

In contrast to damaging materials, for which the appearance of a shear band remains today a poorly understood phenomenon,[10] catastrophic rupture of plastic specimens is well explained by the localization (or bifurcation) theory[11-13], as shown in the remarkable analogic[14] experiment of **Fig. 5**.

The analogic material consists in a pack of rolls, the axes of which are perpendicular to the plane. On each roll a T is drawn pointing initially upwards. The structure is then biaxially loaded. As shown in Fig. 5, localization takes place by rotation of the rolls along the two diagonals. Elsewhere rotations remain small. Furthermore, this localization induces a strong dilancy, well marked along the lateral faces of the analogic sample. With the number of contacts decreasing during the localization, the hardening energy blocked up during the loading phase is released. By contrast to damaging geomaterials, for ductile rocks, dilancy appears in a later phase correponding to the collapse of the global structure and not to a volumetric damage.

Examples of Elastoplastic Laws

This section succinctly presents two classical elastoplastic models commonly used in geomechanics: the Cam-Clay and the Laderock. They are both written in terms of Terzaghi effective stress.

Modified Cam-Clay Model. The Cam-Clay model[15,16] introduced during the 1960's by Roscoe and Burland is based on the existence of a single plastic mechanism with an associated plastic flow rule. In the P-Q diagram (mean effective stress, stress deviator), the yield locus is an ellipse (**Fig. 6**), the size of which evolves exponentially with the volumetric plastic strain. Physically, this model only reproduces the consolidation mechanism (phase 3 of Fig. 3).

While only considering a purely collapse mechanism, the Cam-Clay includes a false shear failure (the line $Q = MP$ is not a yield locus) corresponding to an ideal plasticity plateau in the stress/strain diagram. It is called critical state line. The main drawback of the Cam-Clay is that it integrates plastic collapse and shear failure in a single mechanism (the ellipse is a function both of effective mean stress and deviator). However, it contains only four physical constants to be experimentally measured. Cam-Clay is well-adapted to cohesionless geomaterials (unconsolidated sands or soft clay—**Fig. 7a**), but does not reproduce the behavior of structured soft materials like chalk or consolidated shales very well (**Fig. 7b**). In the case of Fig. 7b the test is performed under undrained conditions. The pres-

Copyright 1997 Society of Petroleum Engineers

Original SPE manuscript received for review 31 January 1995. Paper peer approved 10 January 1997. Paper (SPE 28058) first presented at the 1994 SPE/IRSM Eurock held in Delft, The Netherlands, 29–31 August.

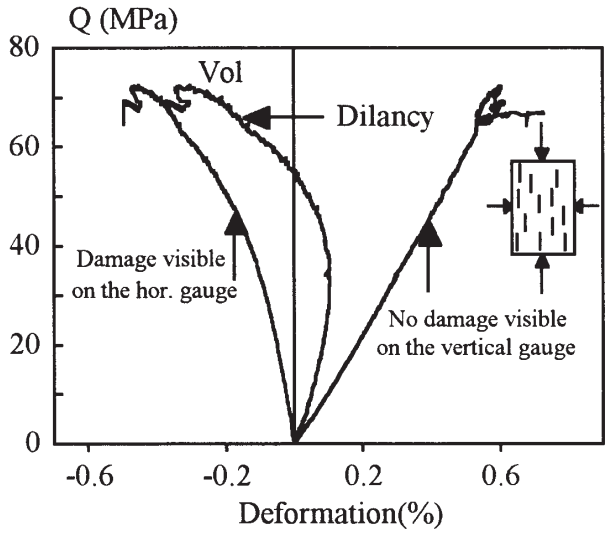

Fig. 1—Typical damaging material (Indonesian sandstone).

ence of a peak in the stress/strain diagram can be interpreted in terms of cohesion. The latter strongly affects the back curve of the *P-Q* diagram; the increase of the interstitial pressure caused by the undrained response is much smaller compared to that predicted by the Cam-Clay, which overestimates the material contractance.

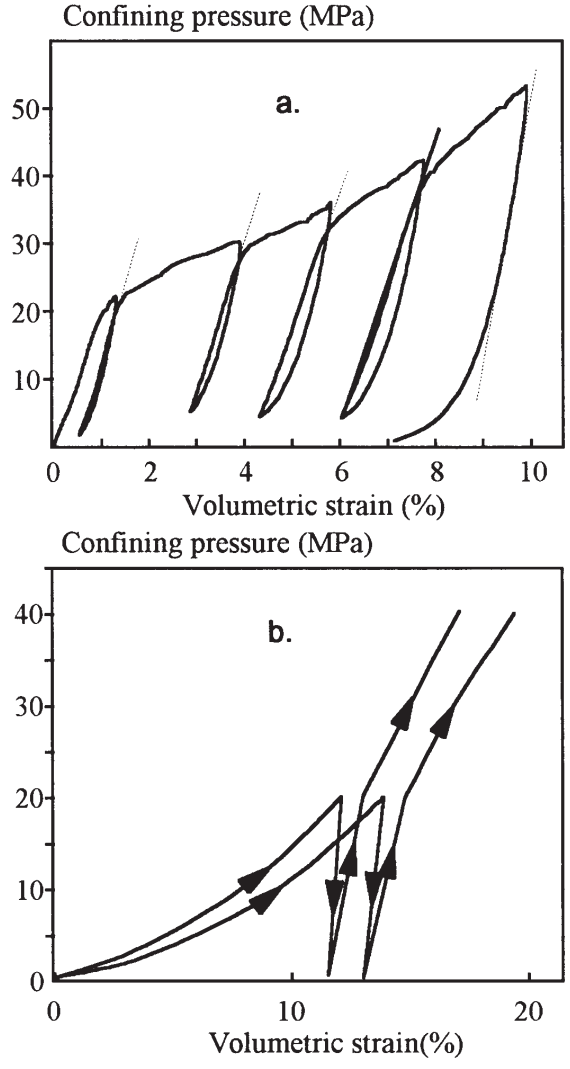

Fig. 3—Example of plastic collapse on soft porous rocks: North Sea chalk (a), Orenico sand (b).

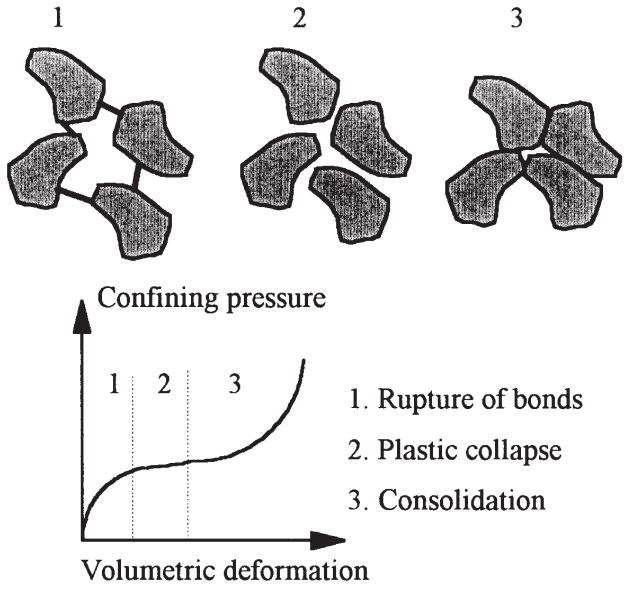

Fig. 2—Plastic collapse of a soft geomaterial.

Laderock Model. The Lade model[17-19], modified by Shao *et. al*[20], is an elastoplastic constitutive law with two independent plastic mechanisms: plastic collapse and shear failure. In the stress space, plastic collapse is described by a plane and is written in terms of the mean effective stress only (**Fig. 8**). In the Laderock model, the hardening law is the product of a power law and an exponential so that it is able to simulate both pore collapse and consolidation phase as shown in **Fig. 9** for Gorm chalk. The deviatoric plastic mechanism is a function of the first and third invariants and is represented in the *P-Q* diagram by a convex curve (Fig. 9), evolving with loading through a hardening mechanism that can modify the curvature of the curve. By contrast, to collapse the shear mechanism integrates a rupture threshold (ultimate value of the curve). Because of its more complex form, Laderock contains eight plastic parameters. One can observe in **Fig. 10** that the Laderock is able to reproduce the complex behavior of a structured clay.

The Wellbore Boundary Problem in Elastoplastic Materials

Analytical Solutions. Numerous elastoplastic solutions of the wellbore boundary problem have been developed in the past.[21-23] Two conditions are required to obtain an analytical solution of the prob-

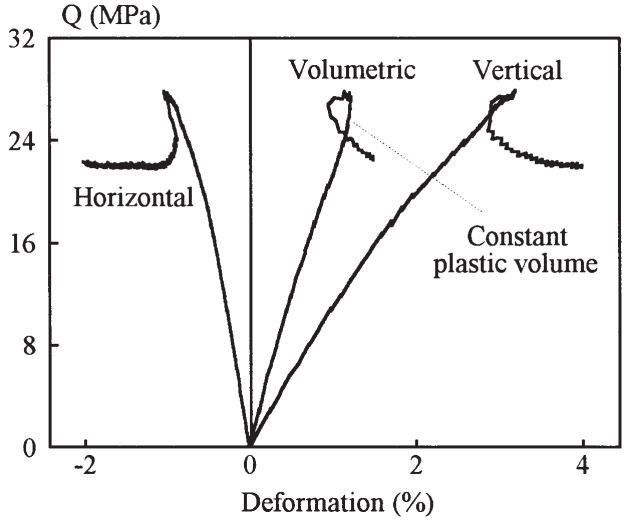

Fig. 4—Example of shear failure in a ductile rock (Villeperdue shale).

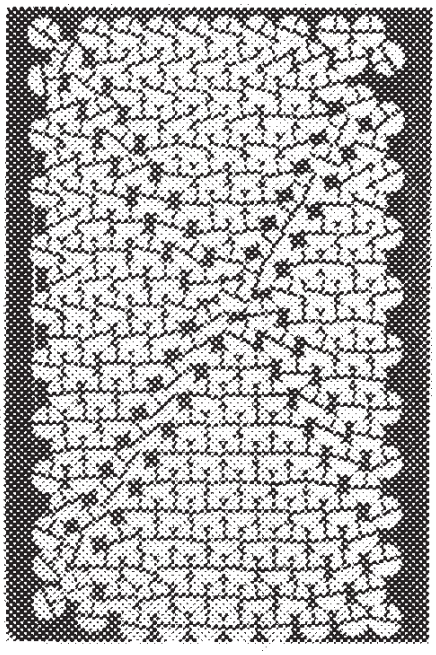

Fig. 5—Analogic experiment showing how a shear band appears in a ductile geomaterial (after Biarez 1990).

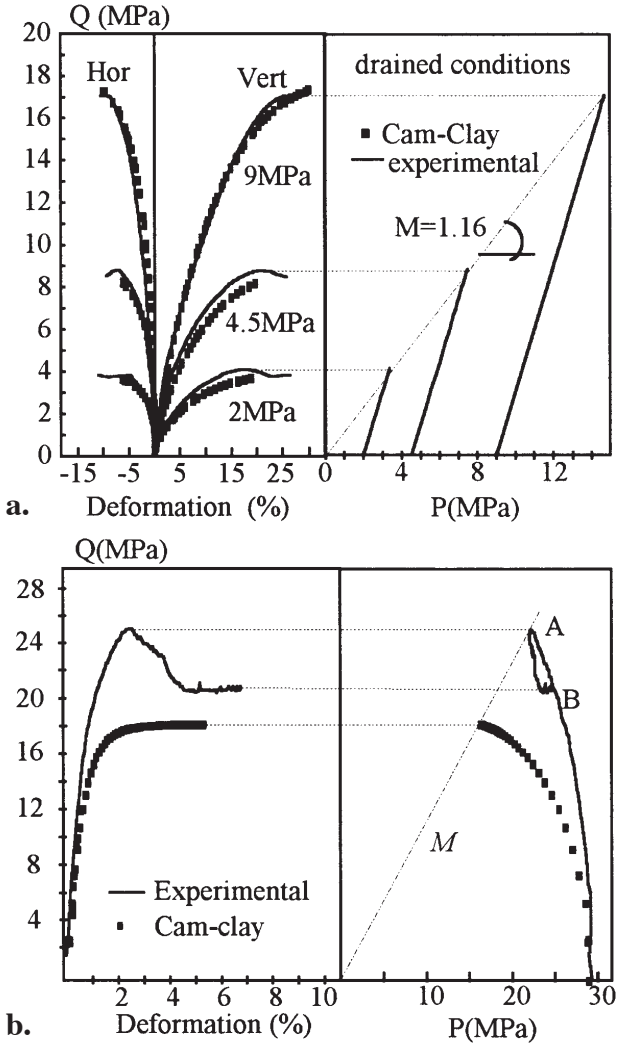

Fig. 7—Validation of the modified Cam-Clay model on an unconsolidated sand (a) and a structured clay (b).

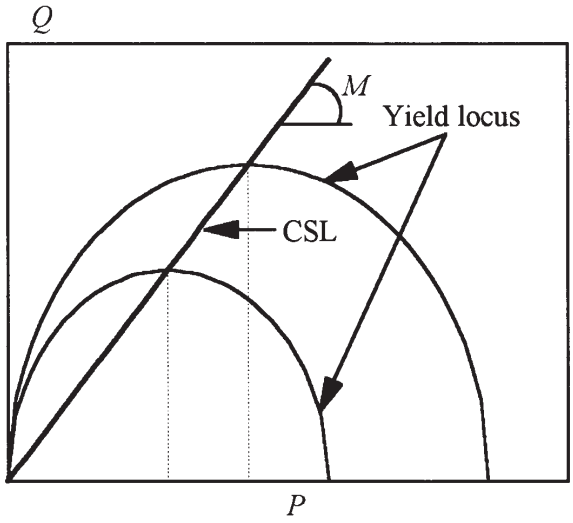

Fig. 6—Cam-Clay model, where CSL is the critical state line..

lem. First, because the state of stress is not calculated with the same equations in elastic and plastic zones, the shape of the plastic zone must be known a priori. In the case of a wellbore, it will only be possible for plane strain axisymmetric cases (horizontal isotropic stress field σ_h and well pressure p_w), for which the potential plastic zone will be an inside ring of radius R_p (**Fig. 11**). However, for anisotropic stress states, with the shape of the plastic zone being unknown, the problem will have to be solved numerically.

Second, to be integrated, the constitutive relations will be linear (linear relationship between stress and strain; linear hardening law). The choice of a linear constitutive law and the knowledge of the shape of the potential plastic region make the plastic wellbore problem (implicit in the general case) an explicit problem. It is important to note that the conditions at the elastic/plastic boundary must respect the continuity of the radial displacement (derived in the compatibility equation) and the radial stress (derived in the equilibrium equation).

Effect of Plasticity and Hardening on Stresses. Some results of a recently developed analytical solution are presented below.[24] The constitutive law is a fully linearized Cam-Clay.

Compared to a purely elastic solution, a strong relaxation of the hoop stress is observed in the plastic zone (**Fig. 12**). By contrast, the radial stress (for which the value is imposed at the two boundaries) is only slightly affected.

From a general viewpoint, plastic hardening plays in favor of stability (**Fig. 13**). The more the hardening modulus, the less the hoop-stress relaxation will be. Following the value of the hardening modulus, the hoop stress exhibits a peak or decreases monotonically.

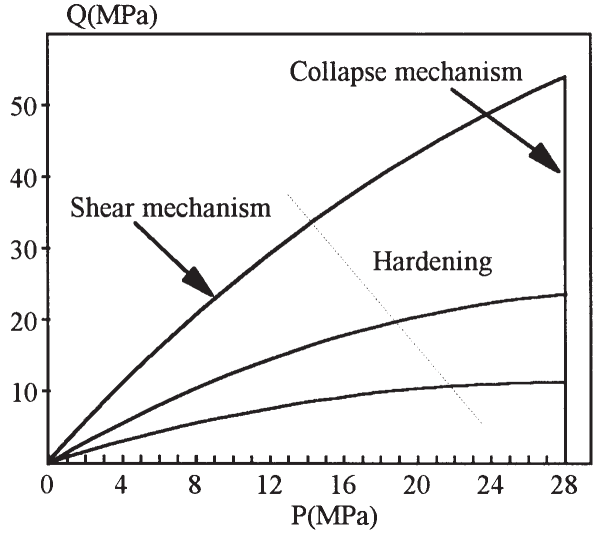

Fig. 8—Yield locus of the Laderock model.

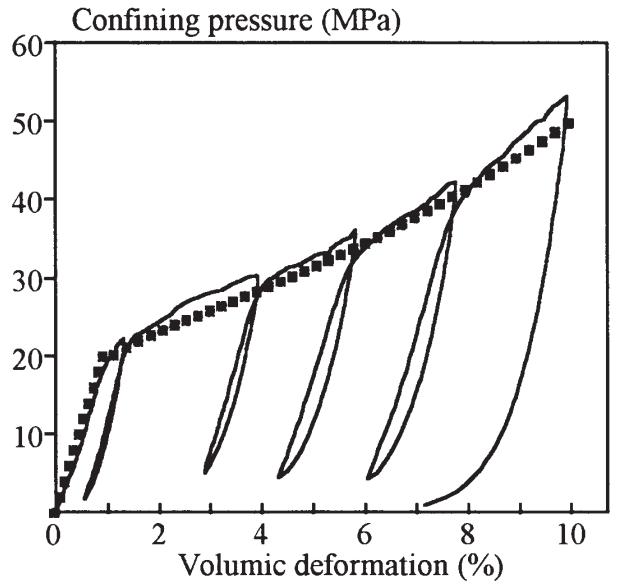

Fig. 9—Validation of Laderock on Gorm chalk (collapse mechanism only).

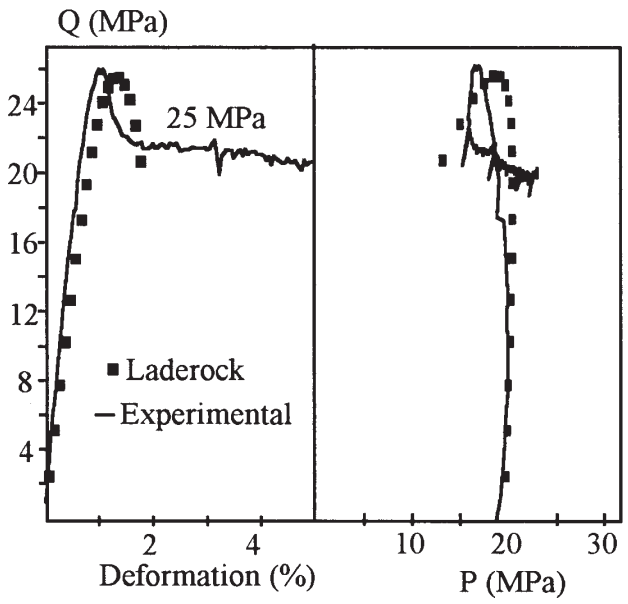

Fig. 10—Validation of Laderock on a structured clay (undrained conditions).

In fact, the elastic model can be considered as the limiting case of an elastoplastic model, for which the hardening modulus is infinite. For this reason, the elastic solution will always be much more pessimistic and will largely overestimate the critical density.

Fluid Coupling—Undrained Response. For a rock saturated by a single fluid of bulk modulus K_f, the undrained pore pressure response prevailing just after the well has been drilled is such that[25]

$$p - p_R = B\frac{\Delta\sigma_{kk}}{3} + \frac{K_f}{\phi_0}\varepsilon^p_{kk} \quad \ldots\ldots\ldots\ldots\ldots\ldots\ldots\ldots \quad (1)$$

where p_R is the virgin pore pressure, B the Skempton's coefficient, $\Delta\sigma_{kk}$ the variation of mean stress, ϕ_0 the porosity, and ε^p_{kk} the volumetric plastic strain. For a poroelastic material[26-28] ($\varepsilon^p_{kk}=0$) and an axisymmetric infinite geometry ($\Delta\sigma_{kk}=0$), no pore pressure response will be observed under undrained conditions. By contrast, for a poroplastic material, a low fluid compressibility increases the value of the hoop stress and plays a negative role on stability (**Fig. 14**).

Numerical Solutions. Analytical solutions can no longer be obtained for nonhydrostatic stress fields and nonlinear elastoplastic laws. This is the case for Cam-Clay or Laderock. The numerical method generally used will be finite elements.[29-32]

With the response to an elastoplastic model being very sensitive to the stress path, the simulation will impose loading steps close to those actually followed. The process will be initiated with a well pressure restoring a state of stress as close as possible to that existing before drilling. The pressure applied at the well will then be decreased under undrained conditions. The calculations presented below are performed with an impermeable well (perfect cake or oil-based mud in contact with a formation saturated with water).

Stress distributions obtained both with Cam-Clay and Laderock (undrained conditions) for a horizontal well are presented in **Fig. 15**. The two constitutive laws are calibrated on the same material.

Qualitatively, the results are similar to those issued from the analytical solution; the radial stress is slightly affected, whereas the hoop stress is strongly relaxed in the vicinity of the well and exhibits a peak well-marked inside the formation. However, we should note that the hoop-stress relaxation is larger with the Laderock.

Undrained Response. In the case of a nonhydrostatic stress field, with the mean stress increasing in the direction of σ_h, according to Eq. 1 in Ref. 1, the undrained pore pressure response will induce an overpressurized zone along the x-axis.[33,34] As shown in **Fig. 16,** the location of this zone is strongly affected by the compressibility of the saturating fluid. The volumetric plastic strain is always maxi-

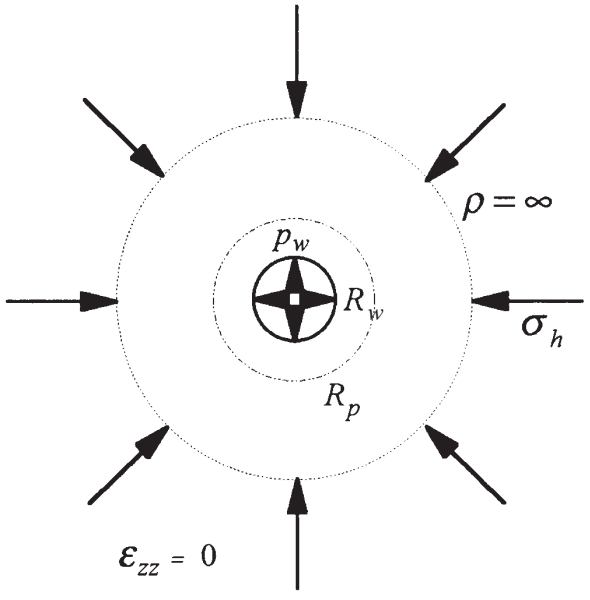

Fig. 11—The axisymmetric wellbore boundary problem.

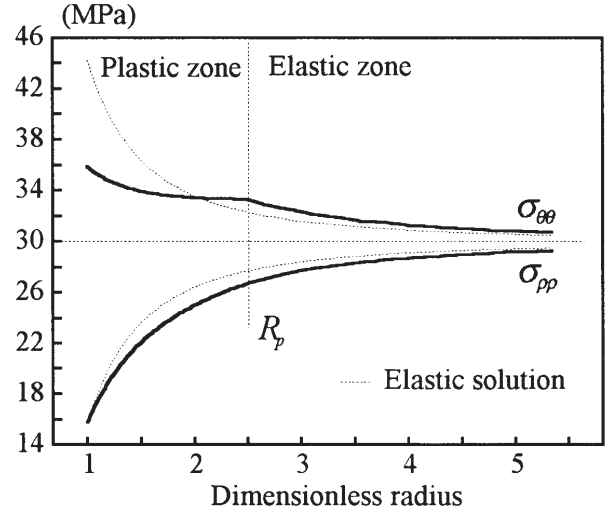

Fig. 12—Comparison of plastic and elastic solutions.

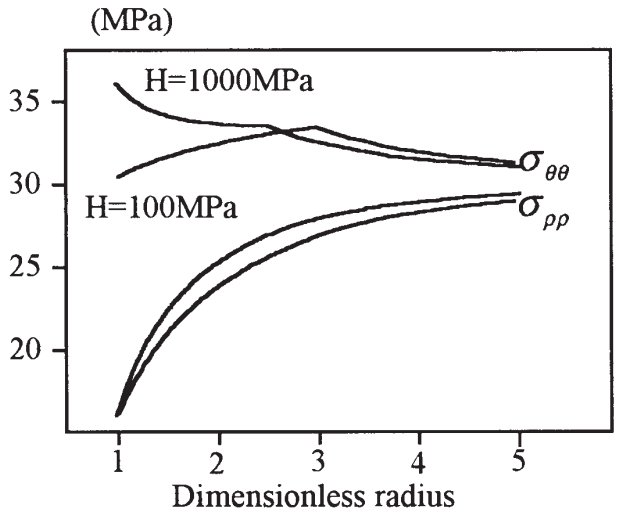

Fig. 13—Effect of strain hardening on the state of stress around a wellbore.

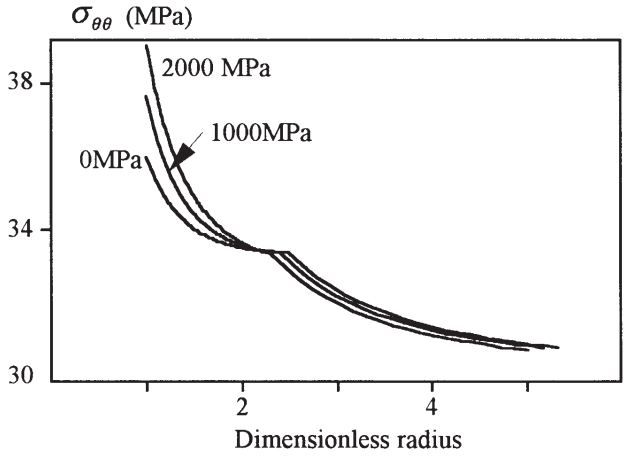

Fig. 14—Undrained pressure response in a linear strain hardening material for different values of fluid compressibility, k_f.

mum at the well, but the mean stress (depending on the hardening parameters) can be maximum either at the well or inside the formation. Consequently, depending if the saturated fluid is, for instance, gas or water, the maximum pore pressure can be observed either at the well or inside the formation.

Drained Response. Assuming the well is impermeable, the effect of time consists in a diffusion process corresponding to a regularization of the undrained solution; the fluid flows from the overpressurized zone (parallel to the minor stress) to the underpressurized zone (parallel to the major stress).

Fig. 17 shows the progressive attenuation of the initial pore pressure peak (water-saturated rock), which with time is displaced inside the formation.

How To Switch From the Boundary Problem to the Wellbore Stability Problem

Criterion of Decision Based on Local Action Principle. The boundary problem allows calculating stresses around the structure, but it does not give any type of information about stability. One has to add a criterion of decision to stress considerations. The most simplistic type of criterion is based on the local action principle.[35,36] The structure is assumed to remain mechanically acceptable until a scalar value (generally combining stresses or strains) oversteps a limit in a point. This limit can be based on experimental considerations (peak ideal-plasticity plateau), or eventually on a bifurcation analysis.[37] Such a criterion is always very subjective; the fact that in a single point, the material loses its resistance (in a broad sense) does not signify that the global structure becomes unstable. A criterion based on the local action principle will always be pessimistic and will overestimate the critical density.

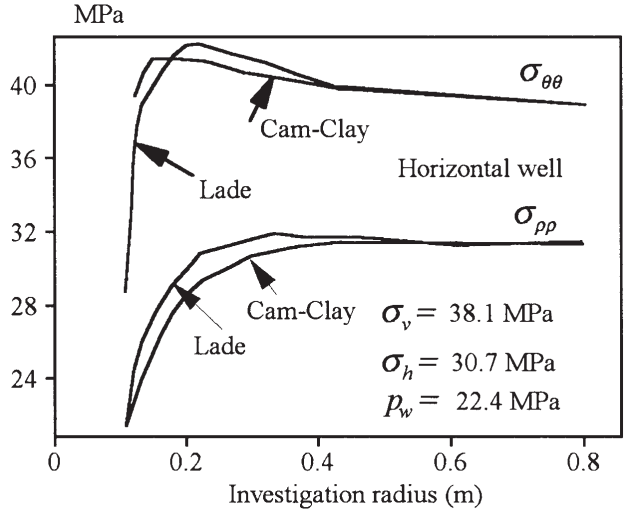

Fig. 15—Stresses obtained by Cam-Clay and Laderock models in undrained conditions (code CESAR LCPC).

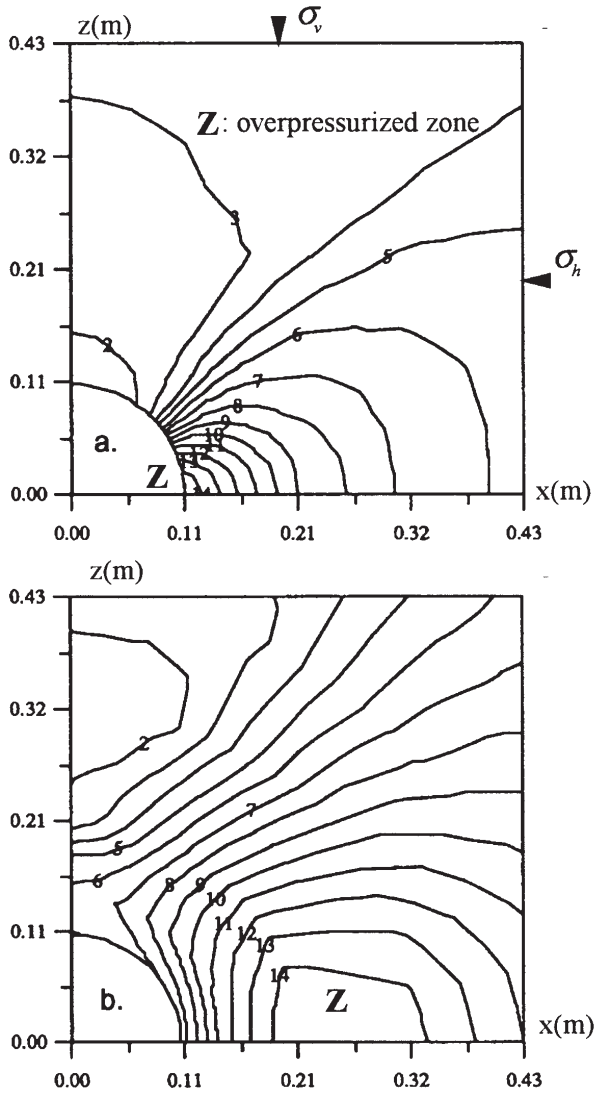

Fig. 16—Pressure distribution in a gas (a) and a water (b) saturated Cam-Clay materials.

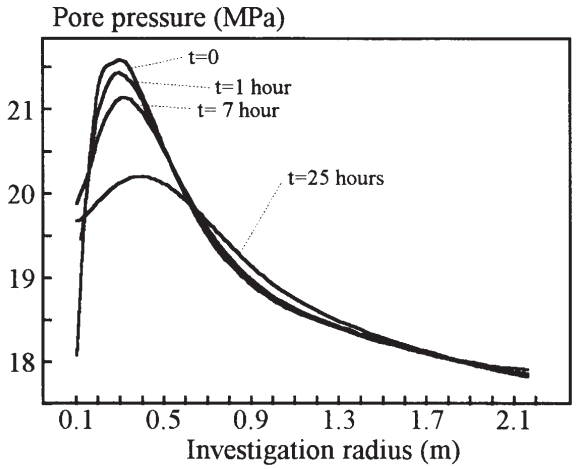

Fig. 17—Evolution of the pore pressure with time (Cam-Clay—water saturated).

Criterion of Decision Based on Bifurcation of the Structure. Another type of approach, which we will mention only briefly, is to appreciate the instability at the scale of the structure itself. This type of approach, based on a follow-up of the localization[38], remains very complex from a numerical viewpoint but is certainly one of the main issues for the future to improve stability predictions.

Critical Instantaneous Mud Weight and Critical Openhole Time

To appreciate the stability of a well, two types of calculations must be performed successively. The first consists of decreasing the mud weight (i.e., well pressure) under undrained conditions until the criterion is reached. The corresponding density is called critical instantaneous mud weight (CIMW). The second phase consists of carrying out a calculation at a constant mud weight (just above the CIMW) under drained conditions to appreciate the effect of time (through a diffusion effect), until the considered criterion is reached again. The corresponding time is called critical openhole time (COHT).

The calculations presented below were performed by using the Cam-Clay model and a local criterion based on the critical-state concept. In the water-saturated overburden (**Fig. 18a**), the rupture zone is located inside the rock, whereas in the gas reservoir (**Fig. 18b**), rupture first appears at the wellbore wall. These results, related to the pore-pressure distributions, show the great importance of poroplastic couplings on wellbore stability.

The results presented in **Fig. 19** (Nuggets reservoir) clearly show that the elastic approach (using a Mohr-Coulomb criterion) is much more pessimistic than the Cam-Clay, which gives a CIMW equal to 1.1 (value perfectly in accordance with densities actually used in the field).

Finally, **Fig. 20** shows the evolution of the most critical point (located at the well in the case of the reservoir) during the first hour of drainage. In that particular case time plays against stability, but this result (clearly related to the undrained pressure distribution of Fig. 16b) will not have to be generalized.

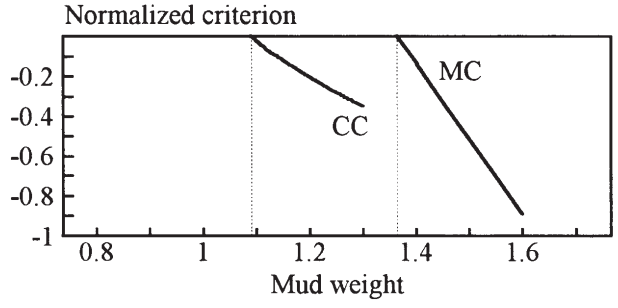

Fig. 19—Estimation of the critical instantaneous mud weight (Nuggets reservoir—vertical well), where CC is Cam-Clay and MC is Mohr-Coulomb.

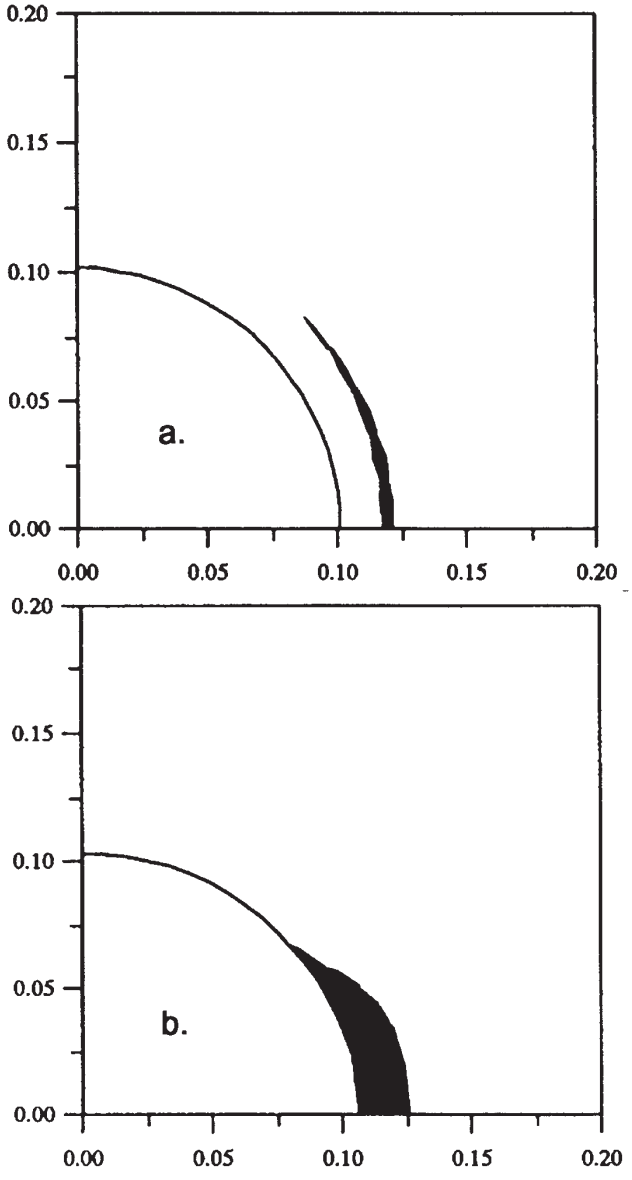

Fig. 18—Location of the rupture zone in the overburden (a) and the reservoir (b) of the Nuggets field (undrained conditions).

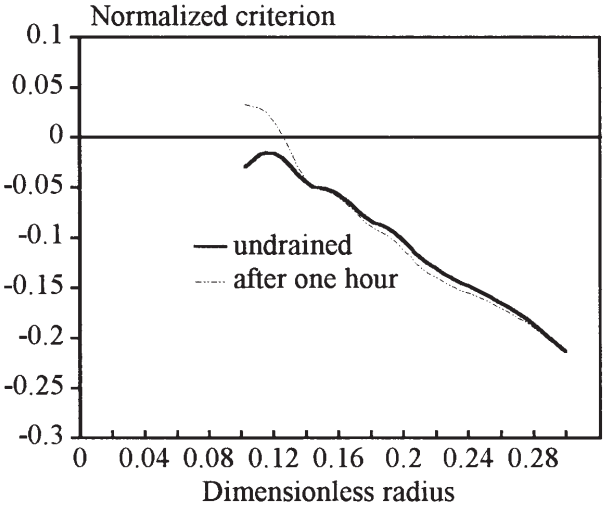

Fig. 20—Evolution of the rupture zone with time (Nuggets clay).

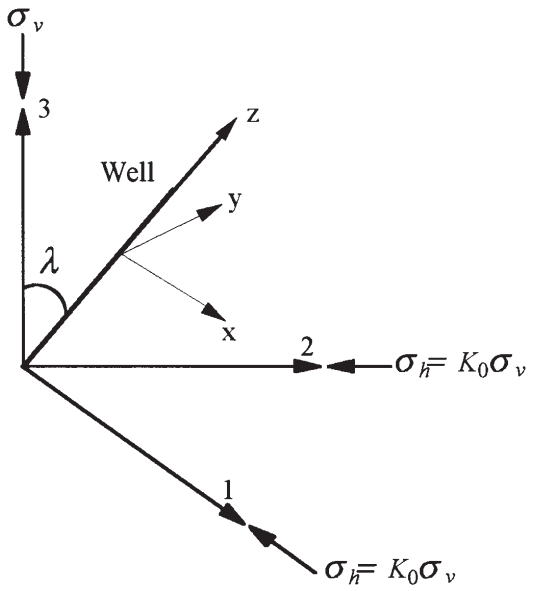

Fig. 21—Deviated well in a nonhydrostatic stress field.

Effect of Deviation and Stress Ratio K_0

Let us consider a deviated well (deviation λ with respect to the vertical—**Fig. 21**) in a nonhydrostatic stress field σ_v, where $\sigma_H = \sigma_h = K_0 \sigma_v$. With respect to a reference frame *x, y,* and *z* linked to the well, the state of stress before drilling in the *x, y* plane is written[21]

$$\sigma_{xx} = K_0 \sigma_v \qquad \sigma_{xy} = 0$$

$$\sigma_{yy} = \sigma_v \left(K_0 \cos^2 \lambda + \sin^2 \lambda \right). \quad \ldots\ldots\ldots\ldots\ldots\ldots \quad (2)$$

Considering a linear elastic dry material ($\sigma_{\theta\theta} = 3\sigma_{yy} - \sigma_{xx} - \rho_m g z$, $\sigma_{\rho\rho} = \rho_m g z$) and a Mohr-Coulomb criterion ($\sigma_{\theta\theta} = C_0 + q\sigma_{\rho\rho}$) the critical mud weight can be easily calculated

$$\left(\frac{\rho_m g z}{\sigma_v} \right)_{cr} = \frac{\left[3 \sin^2 \lambda + K_0 (3 \cos^2 \lambda - 1) - C_0 \right]}{q + 1} . \quad \ldots\ldots\ldots \quad (3)$$

The set of curves is clearly divided in two parts (**Fig. 22**). For low deviations, the critical density increases according to K_0. A high K_0 value has thus a negative effect on stability. However, for high deviations, the critical density decreases with respect to K_0, which will favor stability. These results lead to important conclusions. First of all, the K_0 coefficient in Eq. 2 is nullified for a deviation equal to 54.7°. This theoretical value, called neutral deviation, is insensitive to K_0. Secondly, deviated wells in the range of 30 to 50° require large increases of mud weight to be stabilized, particularly at low K_0 values. However, above the neutral deviation (roughly 50 to 90°), the curve strongly flattens and only a small additional increase in mud weight will ensure stability.

Field Example

Let us try now to compare critical instantaneous densities with actual field densities. This comparison is not always objective, because actual field densities are not imposed only with respect to stability considerations. On the other hand, field densities can correspond to a mechanically unstable well that is without drastic drilling problems. In that case, the feeling of the driller (who considers that the mud weight is sufficient) will be in opposition to that of the geomecanician (who considers the well unstable). Density alone is too subjective; other measurements such as caliper should be added to appreciate the prediction of the model.

Presented below is a database including 60 wells of the Villeperdue field (Callovian of the Bassin de Paris). This level (a marl) is crossed (for any deviation) with mud weights between 1 and 1.2. Using an odometric initial state of stress ($K_0 = 0.63$), and a hydrostatic hypothesis for the virgin pore pressure, the Cam-Clay model

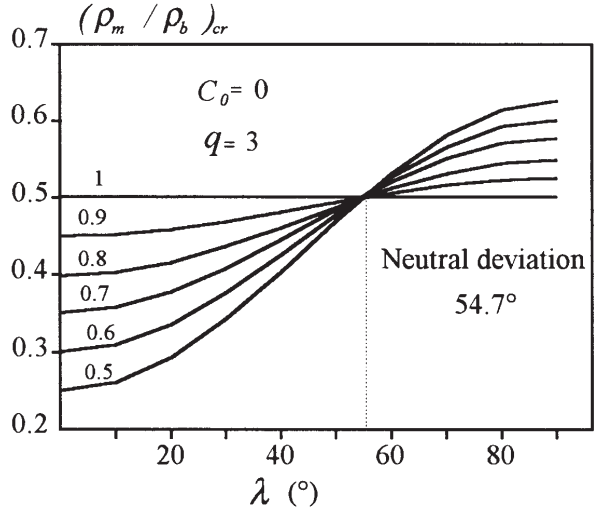

Fig. 22—Effect of K_0 and deviation on critical mud weight.

(calibrated using odometric tests and undrained triaxial tests) gives good predictions for deviations less than 35°, but becomes very conservative for higher deviations (**Fig. 23**).

The excessive effect of the deviation is clearly caused by the value of K_0. An XLOT performed 100 m higher leads to $K_0 = 0.8$. For this value, the critical mud density curve (equal to 1.28 for 90° of deviation) overestimates, but only in a small range the actual mud weights. Let us focus our attention on points 1, 2, and 3 of Fig. 23. Point 1 corresponds to the first horizontal well. For instability reasons, the well was abandoned when crossing the Callovian using a mud weight equal to 1.01. This value (chosen without any stability study) was really too low to cross the Callovian with 65° of deviation and a 12¼-in. well diameter. Points 2 and 3 are the densities used for the next two horizontal wells, using the predictions of the model with an oedometric K_0 (= 0.63). The very pessimistic recommendations allowed performing the wells but at a very high cost. For the next wells, the mud weight was progressively decreased, and finally a value between 1.15 and 1.2 was used. These values are in good accordance with a K_0 between 0.80 and 0.85. It should be noted that the two deviation effects discussed previously are again observed; for small deviations, critical densities increase with K_0, whereas for high deviations, the tendency is inverted. The neutral density here is equal to 35°.

Parallel to densities, the calipers are studied in **Fig. 24**. They show the strong impact of the mud chemistry on the well quality. With an

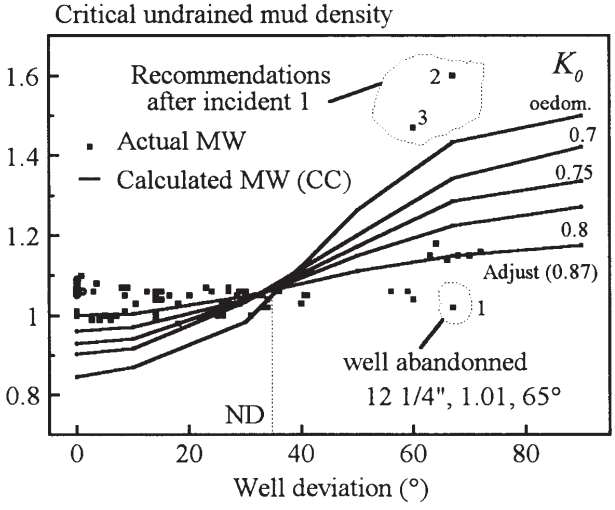

Fig. 23—Comparaison of actual and calculated mud weight (MW).

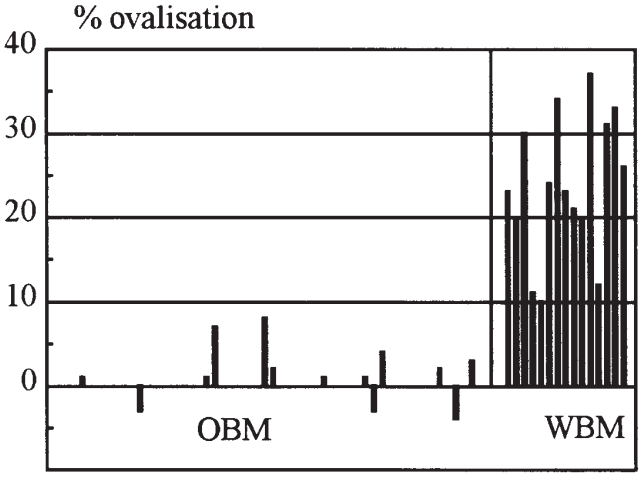

Fig. 24—Intensity of ovalization for oil-based mud (OBM) and water-based mud (WBM).

oil-based mud, the well is always perfectly in gauge, while with a water-based mud, deep caving is observed.

Conclusions

On Constitutive Laws. In the range of confining pressures of several tens of MPa, soft, deep materials clearly exhibit a ductile/plastic behavior with two plastic mechanisms: plastic collapse and shear failure. Elastoplastic models including these two mechanisms separately (Laderock) or together (Cam-Clay) will generally be sufficient to reproduce this type of rheology.

Boundary Wellbore Problem. Around a well, the main effect of hardening plasticity is to relax the hoop stress. This is the fundamental reason why elasticity will always give out-of-range recommendations for plastic geomaterials.

Fully analytical solutions being only obtained for plane strain axisymmetric cases and linear hardening laws, deviatoric stress fields and more complex constitutive laws (Cam-Clay, Laderock) require finite element codes.

Stability Calculations. To give stability recommendations, a criterion of decision shall be added to stress considerations. This criterion, generally based on the local action principle, will give pessimistic recommendations.

Given the fundamental role of the saturating fluid, the wellbore-stability problem shall be solved in the general scope of poroplasticity. Two types of calculations will be systematically performed: undrained calculation (to estimate CIMW) and drained calculation (to estimate COHT).

Most Sensitive Parameters and Effect of Deviation. The initial state (initial stresses and initial pore pressure) is by far the most important. Particularly, the deviation effect is fully contained in the far stress field. At low deviations a large K_0 will play against stability; for high inclinations, the opposite situation will be observed.

Nomenclature

$B =$ Skempton coefficient
$C_0 =$ unconfined compressive strength, MPa
$g =$ gravity acceleration
$H =$ hardening modulus, MPa
$K_f =$ fluid bulk modulus, MPa
$K_0 =$ stress ratio
$M =$ slope of critical state line
$P =$ mean effective stress, MPa
$Q =$ stress deviator, MPa
$p =$ pore pressure
$q =$ friction angle parameter
$R_w =$ well radius, m
$R_p =$ plastic radius, m
$t =$ time
$x =$ Cartesian coordinates
$y =$ Cartesian coordinates
$z =$ Cartesian coordinates
$\varepsilon^p_{kk} =$ mean plastic strain
$\varepsilon_{zz} =$ axial strain
$\lambda =$ well deviation
$\rho_b =$ bulk overburden density
$\rho_m =$ mud density
$\sigma_v =$ vertical stress, MPa
$\sigma_h =$ minor horizontal stress, MPa
$\sigma_H =$ major horizontal stress, MPa
$\sigma_{xx} =$ Cartesian stress, MPa
$\sigma_{xy} =$ Cartesian stress, MPa
$\sigma_{yy} =$ Cartesian stress, MPa
$\sigma_{\theta\theta} =$ hoop stress, MPa
$\sigma_{\rho\rho} =$ radial stress, MPa

Subscript

$cr =$ critical

Aknowledgments

The author expresses his gratitude to Total for allowing publication of this paper. L. Le Gurrun, B. Little, and C. Tan are acknowledged for their help and contribution.

References

1. Nemat-Nasser, S. and Horii, M. (1993): "Micromechanics: overal properties of heterogeneous materials," *North-Holland*.
2. Cheng, H. and Dussault, M.: "Deformation and Diffusion in a Solid Experiencing Damage: a Continous Damage Model and its Numerical Implementation," *Intl. J. Rock Mech. Min. Sci. & Geom. Abst.* Vol. 30, N° 7, December 1993.
3. Brignoli, M. and Sartori, L.: "Incremental constitutive Relations for the Study of Wellbore Failure," *Intl. J. Rock Mech. Min. Sci. & Geom. Abst.* Vol. 30, N° 7, December 1993.
4. Dragon, A., Charlez, P., D. Pham & Shao, J-F.: "A model of anisotropic damage by (micro) crack growth," *Assessment and prevention of failure in Rock Engineering,* Istambul, April 1993, A.A. Balkema.
5. Brace, W.F., Paulding, B.W. and Scholtz, C. (1966): "Dilatancy in the fracture of cristalline rocks," *J. of Geoph. Res.*, Vol. 71, N° 116.
6. Roegiers, J-C. Azeemuddin, M., Zaman, M.M., and Abdulraheem, A.: "A constitutive model for characterizing dilatancy in Rocks," *Proceedings of the 32nd U.S. Symposium Rock Mechanics as a mulidisciplinary science,* Norman, 1991, A.A. Balkema.
7. Lee, M. and Haimson, B.: "Laboratory study of borehole breakouts in lac du Bonnet Granite: a case of extensile failure mechnanism," *Intl. J. Rock Mech. Min. Sci. & Geom. Abst.,* Vol. 30, N° 7, December 1993.
8. Brace, W.F. and Bombolakis, E.G. (1963): *J. of Geoph. Res.*, Vol. 68, 163–242.
9. Charlez, P.A. and Shao, J.F.: "Mechanical behaviour of soft deep rocks," in *Geotechnical Engineering of Hard Soils—Soft Rocks,* Athens, 20–23 September 1993, A.A. Balkema.
10. Charlez, P.A. (1991): "Rock Mechanics—Theoretical fundamentals," Ed. Technips.
11. Rudnicki, J.W. and Rice, J.R. (1975): "Conditions for the localisation of deformations in pressure sensitive dilatant materials," *J. Mech. Phys. Solids*, Vol. 23, 371–394.
12. Vardaoulakis, I. (1979): "Bifurcation analysis of the triaxial test on sand samples," *Acta Mechanica,* 32, 35–54.
13. Tillard, D. (1992): "Etude de la rupture dans les géomatériaux cohésifs. Application à la marne de Beaucaire," *Thèse de l'Université J. Fourier*—Grenoble I.
14. Biarrez, J. and Meftah, A. (1990): "From grains to a continuum," A.A. Balkema.
15. Burland, I.B, and Roscoe, K.H. (1968): "On the generalized stress strain behaviour of wet clay," *In Engineering plasticity,* Cambridge Heyman-Leckie.
16. Loret, B. (1987): "Elastoplasticité à simple potentiel," in *Manuel de Rhéologie des Géomatériaux,* ENPC press.
17. Lade, P.V. (1977): "Elastoplastic stress strain theory for cohesion less soil curved yield surface," *Intl. J. Solid Structures*,Vol. 13, 1019–1036.
18. Lade, P.V (1977): "Prediction of undrained behaviour of sand," *J. of the Geot. Eng. Div.,* June.

19. Lade, P.V. (1978): "Three dimensional behaviour of remoulded clay," *J. of the Geot. Eng. Div.,* Febuary.
20. Shao J.F., Henry J.P. and Guenot, A. (1988): "An adaptative constitutive model for soft porous rocks (Chalk)," *Proceedings of the XXIXth U.S. symposium "Key questions in Rock Mechanics,"* U. of Minnesota, Minneapolis, A.A. Balkema.
21. Jaeger, J.C. and Cook, N.G.W. (1979): "Fundamentals of Rock Mechanics," Chapman et. al., London.
22. Risnes R., Bratli R.K., and Horsrud (1982): "Sand stresses around a wellbore," *SPEJ,* 22, 883.
23. Grazziani, A. and Ribacchi, R.: "Critical conditions for a tunnel in a strain softening rock," *Assesment and Prevention of Failure Phenomena in Rock Engineering,* Istambul, April 1993, A.A. Balkema.
24. Charlez, P.A (1997): "Rock Mechanics. Vol II Petroleum Applications," Ed. Technip. In Press.
25. Coussy, O. (1991): "Mécanique des milieux poreux," Ed. Technip.
26. Rice, J.R. and Clearly, M.P. (1976): "Some basic stress diffusion solutions for fluid saturated elastic porous media with compressible constituents," *Rev Geoph. Space Phys.,* 14 227–241.
27. Detournay, E., and Cheng, A. (1988): "Poroelastic response of a borehole in a non hydrostatic stress field," *Intl. J. Rock Mech. Min Sci & Geom Abstract,* 25 171–182.
28. Charlez, P.A. (1995): "The well and Termoporoelasticity," *In. Mechanics of Porous Media,* Ph. Charlez, Ed A.A. Balkema.
29. Detournay, E. (1986): "Elastoplastic model of a deep tunnel for a rock with variable dilatancy," *Rock Mech. Rock Eng* 19: 99–108.
30. Veeken, C., Walters, J.V., Kenter, C.J. and Davies, D.: "Use of plasticity models for predicting borehole stability," *Symp. Rock at Great Depth,* Pau, 1989, A.A. Balkema.
31. Ewy, R.T.: "3D stress effects in elastoplastic wellbore failure models," Proceedings of the 32nd U.S. Symposium Rock Mechanics as a mulidisciplinary science, Norman, 1991, A.A. Balkema.
32. Charlez, P. and Heugas, O.: "Evaluation of optimal mud weight in soft shale levels," Proceedings of the 32nd U.S. Symposium Rock Mechanics as a mulidisciplinary science, Norman, 1991, A.A. Balkema .
33. Shao, J.F. and Henry, J.P. (1993): "Application of a poroelastic model to analysis of wellbore stability and reservoir compaction," in *Geotechncial Engineering of Hard Soils—Soft Rocks*, Athens, A.A. Balkema.
34. Aoki, T., Tan, C.P. and Bamford, W.E.: "Effects of Deformation and strength Anisotropy on Borehole Failures in Saturated Shales," *Intl. J. Rock Mech. Min. Sci. & Geom. Abst.*, Vol. 30, N° 7, December 1993.
35. Guenot, A.: "Contraintes et ruptures autour des forages pétroliers," *Proc. 6th ISMR Congr.,* Montréal, 1987.
36. Guenot, A. and Santerelli, F.J. (1988): "Borehole stability: a new challenge for an old problem," *Proc 29th US Rock Mech. Symp.,* Minneapolis, A.A. Balkema.
37. Charlier, R. and Pierry, J.: "Finite element modelling of rock drilling," *Assessment and prevention of failure in Rock Engineering,* Istambul, April 1993, A.A. Balkema.
38. Papanastasiou, P. and Vardoulakis, I.: "Numerical Analysis of Borehole Stability Problem," in *Soil Structure interaction: numerical analysis and modelling,* Edited by J.W. Bull, E&FN SPON.

SI Metric Conversion Factors

ft	×3.048*	E−01 = m
in.	×2.54*	E+00 = cm
lbf/ft^2	×6.894 757	E−03 = MPa

*Conversion factor is exact. **SPEDC**

Philippe A. Charlez is a mining engineer from Ecole des Mines de Mons (Belgium) and has a PhD degree from Inst. de Physique du Globe de Paris. He has been Geomechanics Expert with Total for more than 10 years, and was involved in numerous projects focused on hydraulic fracturing, reservoir compaction, and wellbore stability. Charlez has published more than 30 articles on petroleum rock mechanics. He is also the author of two books. He is currently a senior drilling engineer with Total Oil Marine in Aberdeen.

b&w 1/2
TH Hill & Assocs.

Circle **3** on Reader Service Card